General Disclaimer

One or more of the Following Statements may affect this Document

- This document has been reproduced from the best copy furnished by the organizational source. It is being released in the interest of making available as much information as possible.

- This document may contain data, which exceeds the sheet parameters. It was furnished in this condition by the organizational source and is the best copy available.

- This document may contain tone-on-tone or color graphs, charts and/or pictures, which have been reproduced in black and white.

- This document is paginated as submitted by the original source.

- Portions of this document are not fully legible due to the historical nature of some of the material. However, it is the best reproduction available from the original submission.

STUDY OF LASER HEATED PROPULSION DEVICES

Final Report — Part II

ASSESSMENT OF LASER PROPULSION MODELING AND SIMULATION REQUIREMENTS

by

Jürgen Thoenes

Lockheed
Missiles & Space Company, Inc.
Huntsville Research & Engineering Center
4800 Bradford Drive, Huntsville, AL 35807

Contract NAS8-33974

April 1982

Prepared for

NASA-GEORGE C. MARSHALL SPACE FLIGHT CENTER
MARSHALL SPACE FLIGHT CENTER, AL 35812

FOREWORD

The work described in this report was performed for the Auxiliary Propulsion Branch of the Propulsion Division, Structures and Propulsion Laboratory, NASA George C. Marshall Space Flight Center under Contract NAS8-33974. The NASA technical monitors were Lee W. Jones and T.D. McCay.

This report represents Part II of the Final Report. Part I deals with the evaluation of alternate laser devices as well as alternate propellants and energy coupling schemes.

ABSTRACT

The present status of theoretical models for the laser heated thruster is reviewed. It is concluded that existing models neither agree with each other nor with the limited experimental data available. The requirements for an improved laser heated thruster theoretical model are discussed. The application of a time-dependent finite-difference Navier-Stokes equation solution to the laser heated thruster problem is described, along with a simple closed form solution which was developed in order to gain insight into the difficulties encountered in the pursuit of the numerical solution.

CONTENTS

1. LASER HEATED PROPULSION MECHANISM

The concept of laser heated propulsion is based on using a laser beam to remotely heat a working medium in a rocket thruster. Such a scheme appears to be attractive because it might be possible to generate propellant gas temperatures which are much higher than those possible in chemical propulsion devices. In particular, in conjunction with propellants of low molecular weight, a very high thrust chamber temperature will result in a specific impulse much higher than that achievable in combustion driven rocket motors. Even through the concept is simple, the attendant high temperature presents difficult engineering problems.

The use of continuous wave lasers for laser heated propulsion can be divided into a very high specific impulse, high temperature regime and a high specific impulse, medium temperature regime. While the first regime would be realized by utilizing hydrogen as the propellant and a laser supported absorption wave generated and sustained by inverse bremsstrahlung absorption, in the medium temperature regime laser energy would be coupled into a suitable propellant by molecular or aerosol absorption. Details of these and other schemes are discussed in Part I of this report.

The work described here is mainly concerned with an assessment of laser propulsion fluid mechanics modeling and simulation requirements for the very high specific impulse, high temperature regime. Here the essential feature is that the propellant gas, which is normally a transparent, non-conducting medium, becomes ionized by the laser beam and then strongly absorbs energy from the beam (Ref. 1).

If a few free electrons are present in the focal volume, they can gain sufficient energy from the beam to produce further ionization via collisions

with neutral gas particles. Breakdown will occur if the electron density reaches a critical value despite losses due to diffusion, attachment, recombination and other mechanisms.

Once a plasma has been formed, it emits radiation whose wavelength distribution depends on the temperature and the density. Most of the energy emitted is in the far ultraviolet and is believed to be more readily absorbed in the surrounding cold gas rather than in the plasma itself. Thus, a layer of gas outside the plasma, although transparent to laser radiation, is heated by the plasma radiation, and upon reaching a sufficiently high temperature, will be ionized to such an extent that it will also become absorbing for the laser beam. This layer will then be further heated rapidly until its temperature becomes so high that it in turn will become transparent to ultraviolet plasma radiation. By this time a new layer of plasma nearer the laser will have become absorbing, so the boundary of the plasma, called an absorption wave, will move toward the laser. If this occurs in a flow of propellant gas, the flow velocity of which is equal in magnitude but opposite in direction to the motion of the absorption wave, we have a stationary propellant plasma which can function as the heating mechanism for a propulsion device.

Various laser heated propulsion devices have been conceived and proposed. Since it would be difficult to discuss the modeling and simulation requirements in complete generality, one particular configuration for a laser heated thruster is shown in Fig. 1 (schematically). This is the arrangement used in the subsequent discussion of modeling and simulation requirements. In particular, we are interested in describing or modeling the interaction of the initially cold propellant gas (H_2) as it flows through and around the laser supported plasma region, then mixes and exits through the subsonic-supersonic nozzle, producing thrust in the process.

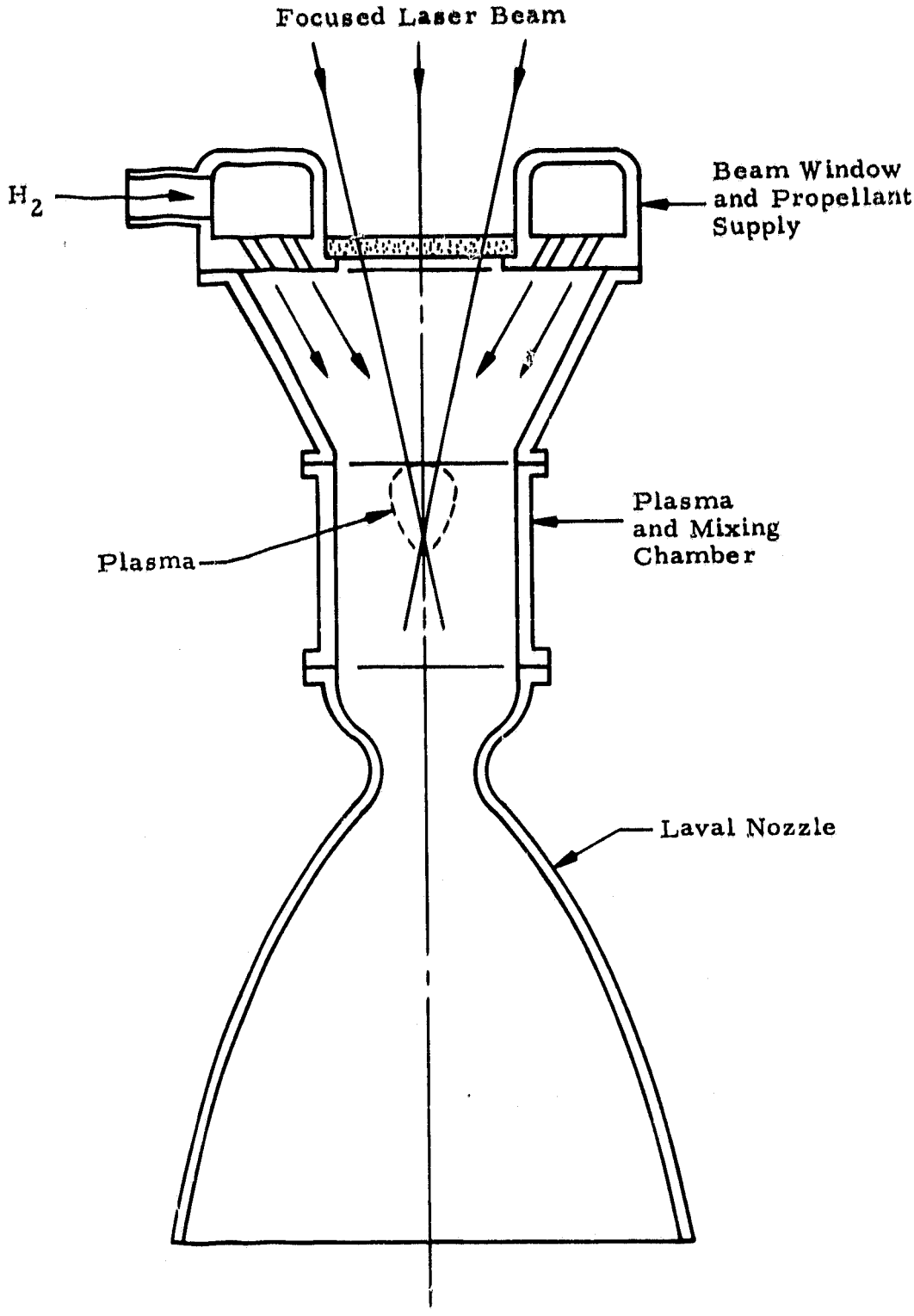

Fig. 1 - Laser Heated Propulsion Device (Schematic)

For the actual design of such a device it is most important to predict the propellant velocity required to achieve a stable plasma as well as the cooling requirements for the plasma and mixing chamber walls. Hydrogen is of particular interest as a propellant because it promises the highest specific impulse.

2. REVIEW OF EXISTING MODELS

2.1 ABSORPTION WAVE MODEL

Although much has been achieved in modeling the physics of the laser heated thruster, much must be done toward obtaining agreement with experiment if these mathematical models are to serve as useful tools in the design of laser heated propulsion devices. Most of the existing models deal with absorption waves in air and have numerous simplifying assumptions in common. Very little work so far has been done with hydrogen as the propellant. Experimental data for absorption waves in hydrogen are also very sparse.

The first model to appear in the literature was that of Raizer (Ref. 2). His model is based on the assumptions of one-dimensional flow at constant pressure with heat conduction considered to be the principal heat transfer mechanism. The plasma is considered to be optically thin to its self-radiance, and in thermal equilibrium. This allows the electron density to be determined from the Saha equation. Also, the absorption coefficient for the absorption of laser radiation via inverse bremsstrahlung as well as an approximate function for the overall radiation losses can be specified as functions of temperature and pressure.

Finally, in order to arrive at an analytical solution, the absorption coefficient as well as the ratio of specific heat to thermal conduction are assumed constant. The neglection of radiation losses limits the applicability of the solution to small plasma volumes (diameters less than a few millimeters at $p = 1$ atm).

With the goal to improve upon the analysis by Raizer, Jackson and Nielsen (Ref. 3) presented a model which includes the mechanism of radiative

transfer into the ambient gas (air). Apart from this, other assumptions made are basically the same as those invoked by Raizer. Jackson and Nielsen derive an analytic solution, the evaluation of which is performed by iterating on the value of the radiative loss function. The authors point out several shortcomings of their analytical solution: (1) interferograms taken of absorption waves show clear evidence of radial flow, rendering the problem two-dimensional, and (2) their calculated propagation velocity of the absorption wave as a function of incident laser intensity does not agree with experiment.

Shortly following the analysis of Jackson and Nielsen, Batteh and Keefer (Ref. 4) presented a two-dimensional generalization of Raizer's analysis for the subsonic propagation of laser sparks in air. To be precise, Batteh and Keefer combined a one-dimensional flow velocity description with a two-dimensional temperature field description, retaining Raizer's assumption of ordinary thermal conduction as the principal propagation mechanism, with plasma radiation serving only as an energy loss mechanism. The importance of this two-dimensional temperature field model is that it provides insight into the effect of boundaries on spark propagation in a channel. Other assumptions such as constant pressure, constant ratio of specific heat to thermal conductivity are also retained. The absorption coefficient was assumed to be piecewise constant, zero in front of the absorption wave, and non-zero within the plasma region. An analytic solution in terms of Bessel functions was obtained to evaluate the relationship between laser intensity and spark propagation velocity.

Batteh and Keefer found that their calculated propagation speeds are roughly an order of magnitude lower than those obtained experimentally, while the maximum temperature in the wave as calculated matched that of the experiment. The authors suggest that this is due to considering thermal conduction only as the primary propagation mechanism. They essentially argue that plasma radiation, causing ionization and additional laser energy absorption via inverse bremsstrahlung in front of the absorption wave must

be included in the model to achieve realistic predictions of the propagation velocity as a function of laser intensity.

The next model, that of Kemp and Root (Ref. 5), in fact does include the effect of forward plasma radiation in a one-dimensional numerical model. This model assumes one-dimensional flow at constant pressure in a constant area channel. Since the equations are solved by numerical integration, it is possible to treat the thermodynamic properties as well as the various transport phenomena (absorption, thermal conduction and radiation) in a much more detailed manner than in the previously discussed analytical solutions. The solution of Kemp and Root's formulation requires an iteration on the mass flux for specified laser intensity. Only one particular mass flux value will yield a physically reasonable temperature distribution in the absorption wave (saddle-point singularity). Calculations are presented for pressures of 1, 3, 10 and 30 atm, and for laser powers of 10 kW and 5 MW. The authors observe a very steep rise in temperature at the leading edge of the absorption wave and caution that for such conditions the "radiation conduction approximation," used to consider the heating effect of plasma radiation on the cold gas in front of the wave, is not really valid. However, since energy is properly conserved in the model, they suggest that the temperature profile in the wave proper should be qualitatively correct. No experimental data for absorption waves in hydrogen were available at the time to confirm the theoretical predictions. Also, the authors realize that the one-dimensional nature of the model presents serious limitations on the validity of the results. It is pointed out that thermal conduction in the radial direction becomes important for small plasma regions at low pressure. A very obvious two-dimensional phenomenon is the focused laser beam. In this case, the intensity will not only change due to absorption but also due to varying cross-sectional area. A convergent beam behaves as a higher intensity beam - relative to a collimated beam of the same initial intensity - and requires a higher propellant flow velocity to keep the "plasmatron" stationary. Finally, there is the transverse velocity component. It is suggested that its effects should be less in a confined flow - such as in a

thruster - than in the unconfined case. Since neither theoretical nor experimental results are available, it is difficult to assess the importance of two-dimensional flow for absorption waves in a channel.

In concluding this brief discussion, it appears that the modeling of absorption waves is still in a stage of infancy. In Fig. 2 (adopted from Ref. 3) we have summarized results for absorption waves in air from the work reviewed here. Some experimental results are also shown. No attempt has been made to systematically correlate these results. It is evident, however, that theoretical predictions are in considerable disagreement with the experimental data (Refs. 6,7) and with each other, even for similar assumptions in the theoretical models.

2.2 THRUSTER AND NOZZLE FLOW MODELS

In order to produce thrust, the heated gas exiting from the absorption wave must be accelerated through a supersonic nozzle which basically converts thermal energy into kinetic energy. Just as for the absorption wave, the modeling of this flow can be approached at different levels of sophistication.

The first of such models to be discussed here is that of Kemp and Root (Ref. 5). It is a one-dimensional model, obtained by explicitly including the area term and retaining the momentum equation in the set of one-dimensional equations used for the one-dimensional absorption wave model by the same authors. The results of the absorption wave calculations serve as initial values for the thruster problem, i.e., the solutions are joined at an appropriate location downstream of the wave. The model described in Ref. 5 represents an "inverse method." In Ref. 5, rather than specifying the thruster and nozzle contour, the velocity is specified as a function of flow distance. While this or variations of this procedure are common in order to avoid the sonic singularity at the throat, it means that many iterations may have to be performed until a reasonable or specified nozzle contour is obtained.

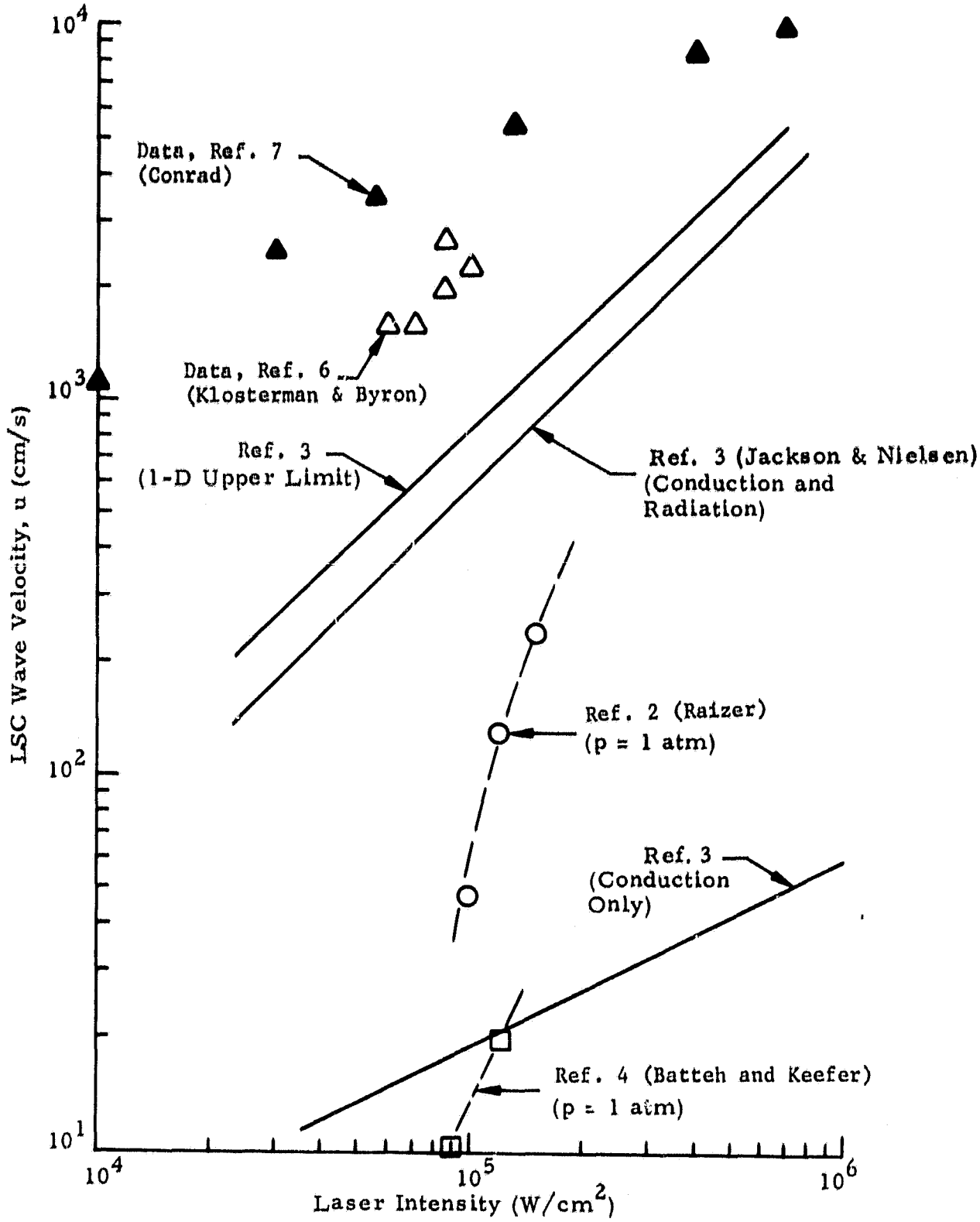

Fig. 2 - Summary of Absorption Wave Velocity Results as a Function of CO_2 Laser Intensity (in Air)

While the one-dimensional thruster flow model has the advantage of simplicity, it cannot properly account for lateral heat condution and radiation to the walls of the thrust chamber. As pointed out in Ref. 5, a precise evaluation of the transverse heat loss due to thermal conduction and radiation requires a two-dimensional model. Such a model was presented by the same author (et al.) in Ref. 8. This model is based on the boundary layer equations and thus includes radial gradients. Added terms for laser energy absorption, equilibrium chemistry and plasma radiation losses complete the equations. Although this model is an improvement over the previously mentioned one-dimensional model, it does not contain any terms for forward energy transport by radiation or conduction, and therefore cannot be applied to model the absorption wave. A method to join the one-dimensional absorption wave calculations to the two-dimensional thruster calculations is described in Ref. 9. According to the authors, the two-dimensional thruster code needs a number of refinements to make it generally useful. Required are a generalization of the radiation model, more experience or a rationale to choose the axial pressure gradient to obtain a desired flow channel contour, and a variable coordinate grid structure to concentrate grid points in areas of steep gradients.

2.3 THERMODYNAMIC AND TRANSPORT PROPERTIES

As compared with other fluid flow problems, the description and analysis of the flow in a laser-heated thruster is severely complicated by the large temperature ranges over which thermodynamic and transport phenomena have to be considered. As a consequence, the early investigations, in particular those that produced analytical solutions, had to employ many simplifying assumptions (Refs. 2, 3 and 4). While the qualitative nature of the results from these analyses is useful in furthering an understanding of the phenomena involved, the pursuit of quantitative results probably demands numerical solutions and much more detailed thermodynamic and transport properties, such as used by Kemp et al. (Refs. 5, 8 and 9). In fact, a substantial portion of the work by Kemp et al. deals with the development, evaluation and assembly of supporting data such as laser absorption coefficients,

as well as thermodynamic and transport properties (conduction and radiation). It is anticipated that any future modeling effort will rely heavily on that work.

While all the existing models so far have assumed thermodynamic equilibrium conditions, it might be necessary to consider nonequilibrium conditions in the future, as pointed out by Batteh and Keefer (Ref. 4) in their discussion of the discrepancy between observed and predicted absorption wave propagation velocities. A calculation of radiative properties of nonequilibrium hydrogen plasma has been presented by Park (Ref. 10) in terms of a computer code which calculates emission and absorption coefficients from given electron temperature, electron density, neutral particle density and intensities of incident radiation. In calculating radiative transport the program shows that there is a large difference between calculated intensities of radiation emitted by a bulk of equilibrium and nonequilibrium hydrogen plasma.

3. THRUSTER MODEL REQUIREMENTS

Based on the preceding discussion of existing models it is now possible to establish the basic features which an improved laser-heated thruster model should incorporate. These features are:

1. Axisymmetric, two-dimensional flow so that effects of radial velocity components can be assessed
2. Axial as well as radial heat transfer, both by thermal conduction and radiation, and
3. Converging (or focused) laser beam configuration to determine the required mass flow more accurately.

Requirement (2) has implications which need further elaborations. It will be shown that this leads to additional requirements.

As previously discussed, the propagation of plasma radiation (VUV) upstream to the front of the absorption wave will likely lead to a non-equilibrium ionization situation. The reason is that electrons have the special property that their particle mass is much less that of any of the other constituents. Because of the inefficiency of energy exchange in elastic collisions between particles of disparate mass, the electron temperature may differ appreciably from the temperature of the heavy particle species (Ref. 11). Additional equations must therefore be included in the model to account for electron mass and energy conservation.

A second, and probably more serious implication of requirement (2) is the fact that the inclusion of upstream influences renders the mathematical problem elliptic. This means that a solution cannot be attempted using a single pass forward marching scheme. Instead, the problem has to be solved considering the entire domain in a time-dependent fashion.

The stated requirements render the potential model more difficult to evaluate than previous models, particularly so if it is visualized that the basic set of equations governing the fluid mechanics (conservation of mass and energy plus the Navier-Stokes equations for conservation of momentum) will have to be solved numerically.

4. MODEL FORMULATION, ANALYSIS AND RESULTS

4.1 DETAILED MODEL FORMULATION

A major goal of this effort was to investigate the effect of two-dimensional fluid mechanics on the conditions in a laser heated thruster by utilizing the available Lockheed GIM code (Ref. 12) which numerically solves the full Navier-Stokes equations (in conjunction with mass and energy conservation equations). Using this code we can therefore satisfy requirement 1, and, as far as thermal conduction is concerned, also requirement 2, as stated in the previous section.

The basic equations for axisymmetric flow as used in the GIM code are:

$$\frac{\partial U}{\partial t} + \frac{\partial E}{\partial x} + \frac{1}{r}\frac{\partial}{\partial r}(rF) + G = 0 \tag{1}$$

where U, E, F and G each represent four components for the equations of conversation of mass, momentum in x- and r-directions and energy as follows:

$$U = \begin{bmatrix} \rho \\ \rho u \\ \rho v \\ \rho \mathcal{E} \end{bmatrix} \tag{2}$$

$$E = \begin{bmatrix} \rho u \\ \rho u^2 + p - \tau_{xx} \\ \rho uv - \tau_{xr} \\ u(\rho \mathcal{E} + p) - u\tau_{xx} - v\tau_{xr} - k\frac{\partial T}{\partial x} \end{bmatrix} \tag{3}$$

$$F = \begin{bmatrix} \rho v \\ \rho uv - \tau_{xr} \\ \rho v^2 - \tau_{rr} \\ v(\rho \mathcal{E} + p) - u\tau_{xr} - v\tau_{rr} - k\frac{\partial T}{\partial r} \end{bmatrix} \tag{4}$$

$$G = \begin{bmatrix} 0 \\ 0 \\ \frac{\partial p}{\partial r} + \frac{\tau_{\theta\theta}}{r} \\ - Q \end{bmatrix} \tag{5}$$

where

$$\mathcal{E} = e + \frac{1}{2}(u^2 + v^2) \tag{6}$$

$$\tau_{xx} = 2\mu \frac{\partial u}{\partial x} + \lambda \nabla \cdot \vec{V} \tag{7}$$

$$\tau_{rr} = 2\mu \frac{\partial v}{\partial r} + \lambda \nabla \cdot \vec{V} \tag{8}$$

$$\tau_{xr} = \mu \left(\frac{\partial u}{\partial r} + \frac{\partial v}{\partial x} \right) \tag{9}$$

$$\tau_{\theta\theta} = 2\mu \left(\frac{v}{r} \right) + \lambda \nabla \cdot \vec{V} \tag{10}$$

and

$$\nabla \cdot \vec{V} = \frac{\partial u}{\partial x} + \frac{1}{r} \frac{\partial}{\partial r}(rv) \tag{11}$$

The above equations represent four equations for the four unknowns - ρ, u, v and T - if we express the pressure through the equation of state as a function of ρ and T, i.e.,

$$p = \rho RT \tag{12}$$

which is valid for a perfect gas. The term Q in the energy equation (see Eq.(5)) denotes the net rate of energy addition to the flow which is represented by the difference between laser energy absorbed and plasma radiation emitted. Since a primary goal was to compare our results with those

obtained from the Batteh and Keefer analysis (Ref. 4), we use their formulation to express Q as

$$Q = \alpha I_o e^{-\alpha x} - m k (T - T_i) \tag{13}$$

where I_o represents the incident laser energy flux of a collimated beam and α is the absorption coefficient. The second term represents a rather crude approximation for the energy loss due to plasma radiation, with the form of this term chosen so as to make the Batteh-Keefer anaytical solution possible (op. cit.).

At the present time, the GIM code is formulated in terms of constant thermodynamic and transport properties. The rather wide range of temperatures of interest in the laser propulsion problem therefore requires us to select suitably averaged quantities for the specific heat, the thermal conductivity and the viscosity. In particular, since we want to compare results with those of Batteh and Keefer, we want to use the same average value for the ratio of specific heat to thermal conductivity that was used in their calculations. For consistency, the same averaging procedure is applied to the gas constant.

Figures 3 through 5 show the thermal conductivity (Ref. 5), the specific heat at constant pressure (Ref. 13) and the molecular weight (Ref. 13), respectively, for equilibrium hydrogen at p = 1 atm as a function of temperature. Integrated averages for c_p, k and the gas constant R are also shown. From these, we can obtain, for use in the GIM code calculations, average values for the ratio of specific heats and the viscosity by applying standard relationships such as

$$\frac{\gamma}{\gamma-1} = \frac{c_p}{R} \tag{14}$$

and

$$k = R\left[\frac{15}{4} + 1.32\left(\frac{c_p}{R} - \frac{5}{2}\right)\right] \mu \tag{15}$$

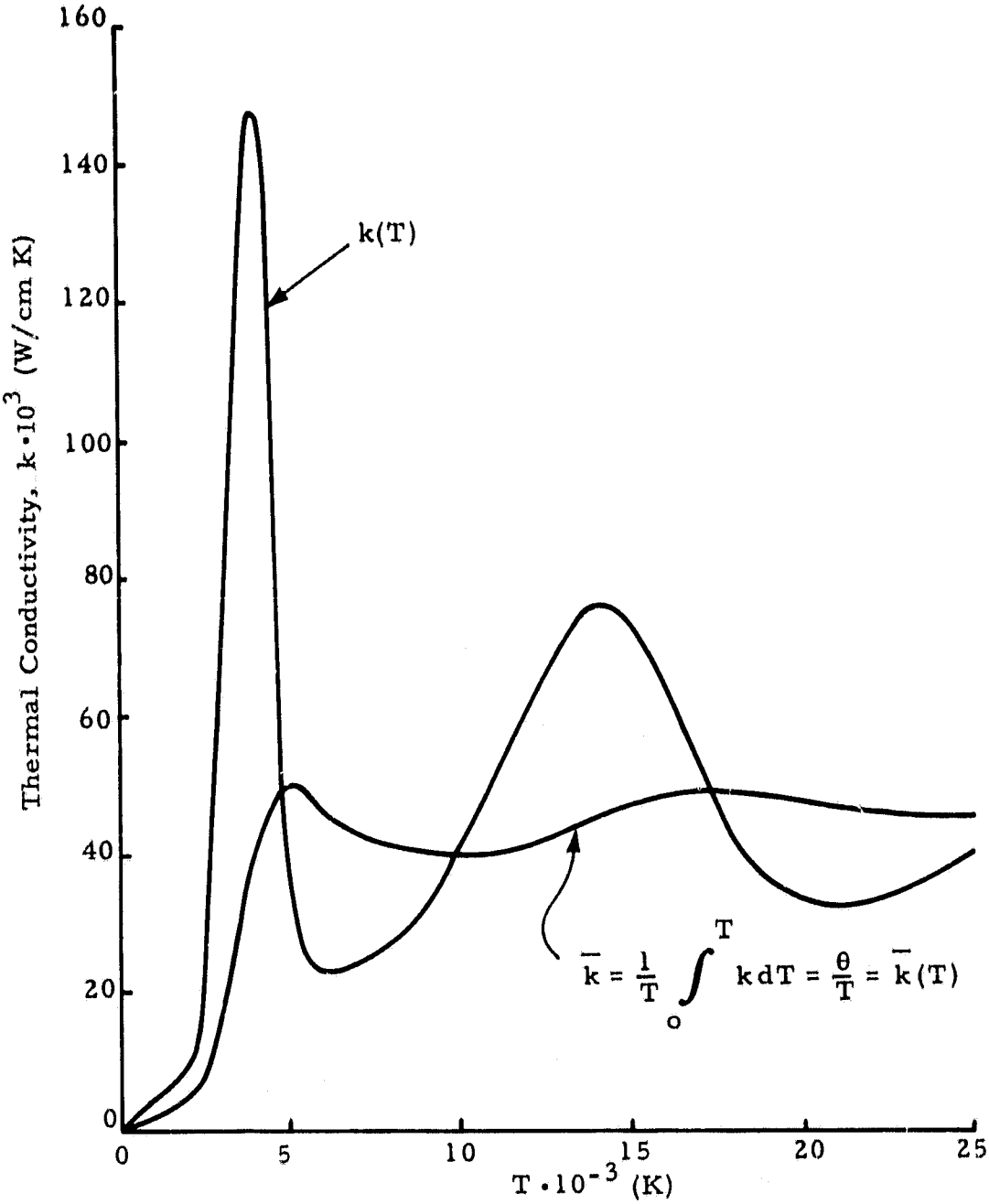

Fig. 3 - Hydrogen Thermal Conductivity (for equilibrium at p = 1 atm, Ref.5)

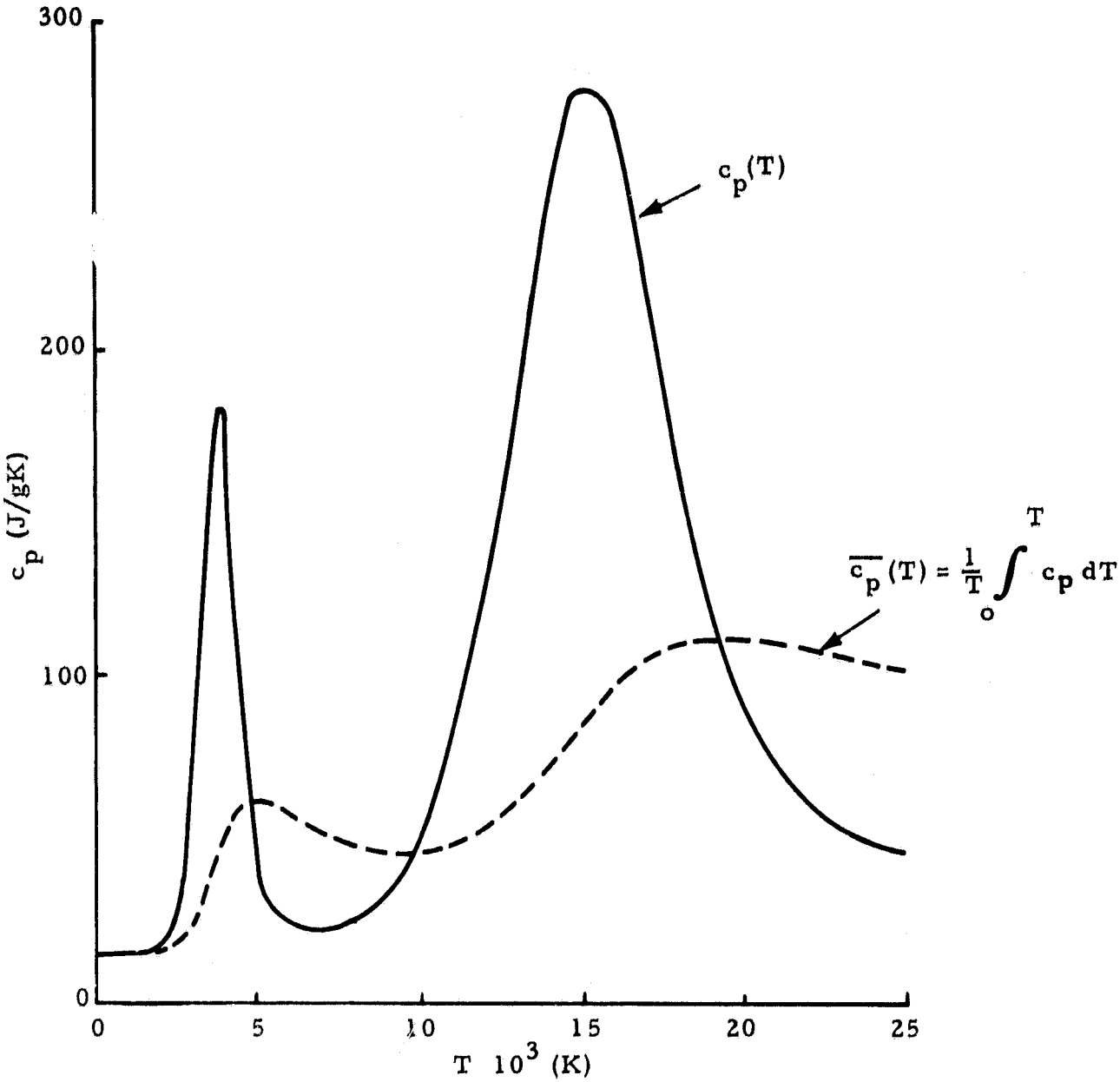

Fig. 4 - Specific Heat of Equilibrium Hydrogen at p = 1 atm (Ref. 13)

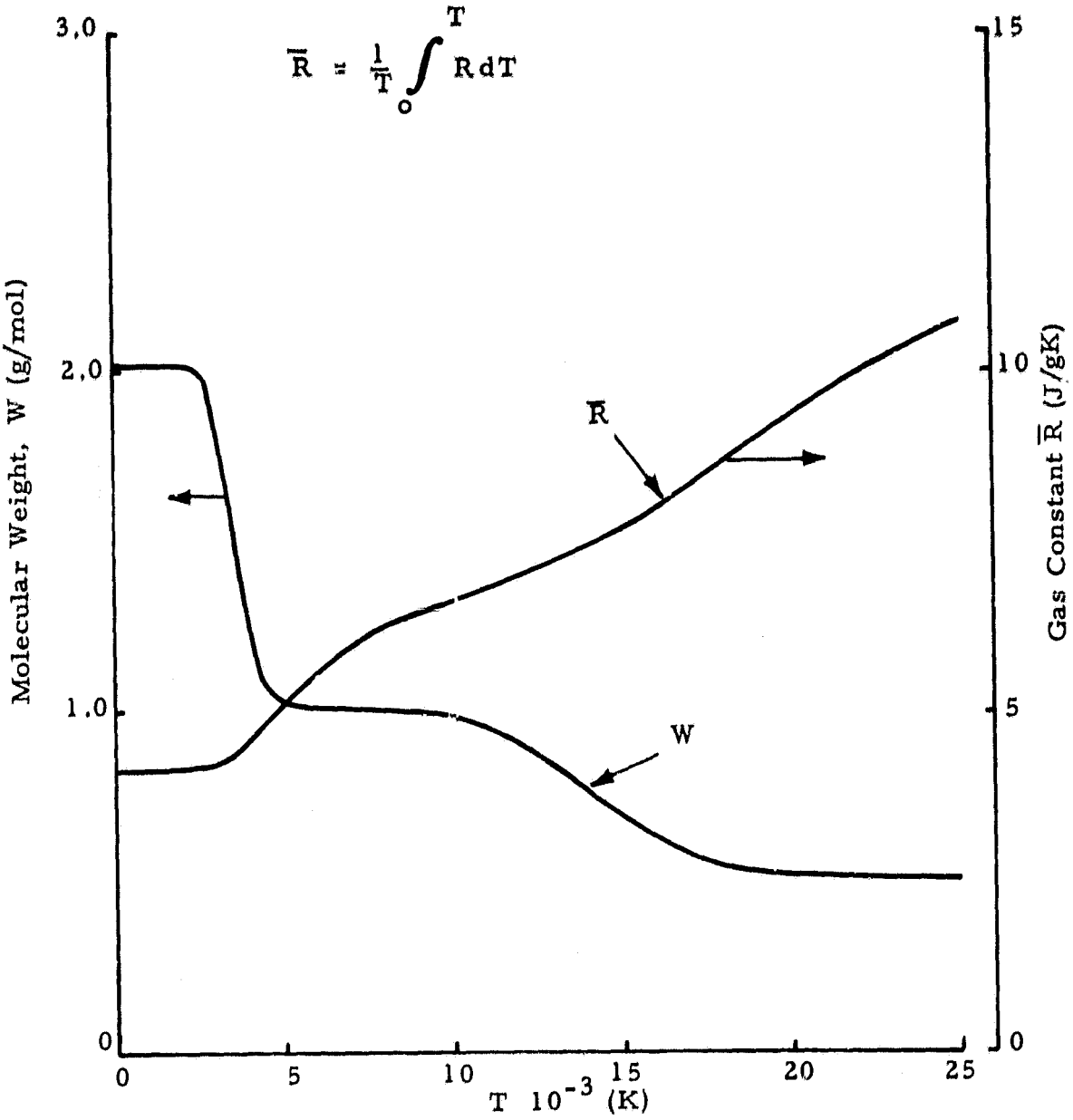

Fig. 5 - Molecular Weight and Gas Constant of Equilibrium Hydrogen at p = 1 atm (Ref. 13)

with the latter taken from Svehla (Ref. 14). Finally, the constant m in the radiation loss function has been evaluated by Keefer et al., to be

$$m = 14.3 \text{ cm}^{-2} \quad (\text{at } p = 1 \text{ atm}).$$

Before we attempt a numerical solution of the full set of equations given in this section, it is useful to investigate possible simplifications. As it turns out, for the contemplated conditions such simplifications are possible. With additional assumptions, this leads to an explicit analytical solution which can easily be evaluated. This will be discussed in the following section.

4.2 A SIMPLE ANALYTICAL SOLUTION

While it is our primary goal to obtain a numerical solution of the full set of equations presented in the previous section, obtaining such a solution will be facilitated by some advance knowledge of what that solution might look like. With this in mind, let us non-dimensionalize the equations by introducing suitable reference quantities for all relevant variables. Defining dimensionless variables as

$$\begin{aligned}
\rho' &= \rho/\rho_o \\
u', v' &= u, v/u_o \\
\mu', \lambda' &= \mu, \lambda/\mu_o \\
\xi, \eta &= x, y/\ell, \; t' = t\, u_o/\ell \\
T' &= T/T_o, \; \mathcal{E}' = \mathcal{E}/c_{vo} T_o \\
c'_v &= c_v/c_{vo} \\
k' &= k/k_o
\end{aligned} \tag{16}$$

and introducing these into the equations, the equations (with primes dropped for convenience) take on the following form:

Continuity:

$$\frac{\partial \rho}{\partial t} + \frac{\partial}{\partial \xi}(\rho u) + \frac{1}{\eta}\frac{\partial}{\partial \eta}(\eta \rho v) = 0 \tag{17}$$

x-Momentum:

$$\frac{\partial}{\partial t}(\rho u) + \frac{\partial}{\partial \xi}\left[\rho u^2 \left(1 + \frac{p}{\rho u^2} - \frac{1}{Re}\tau_{\xi\xi}\right)\right] + \frac{1}{\eta}\frac{\partial}{\partial \eta}\left[\eta\left(\rho uv - \frac{1}{Re}\tau_{\xi\eta}\right)\right] = 0 \tag{18}$$

r-Momentum:

$$\frac{\partial}{\partial t}(\rho v) + \frac{\partial}{\partial \xi}\left[\rho uv - \frac{1}{Re}\tau_{\xi\eta}\right] + \frac{1}{\eta}\frac{\partial}{\partial \eta}\left[\eta\left(\rho v^2 - \frac{1}{Re}\tau_{\eta\eta}\right)\right] + \frac{\partial p}{\partial \eta} + \frac{1}{Re}\cdot\frac{1}{\eta}\tau'_{\theta\theta} = 0 \tag{19}$$

and

Energy:

$$\frac{\partial}{\partial t}(\rho \hat{E}) + \frac{\partial}{\partial \xi}\left[u(\rho \hat{E} + Ep) - \frac{E}{Re}(u\tau_{\xi\xi} + v\tau_{\xi\eta}) - \frac{1}{RePr}k\frac{\partial T}{\partial \xi}\right] + \frac{1}{\eta}\frac{\partial}{\partial \eta}\left\{\eta\left[v(\rho \hat{E} + Ep) - \frac{E}{Re}(u\tau_{\xi\eta} + v\tau_{\eta\eta}) - \frac{1}{RePr}k\frac{\partial T}{\partial \eta}\right]\right\} = \frac{Q}{\rho_o c_{v_o} T_o} \tag{20}$$

where we have defined

$$Re = \frac{\rho_o u_o \ell}{\mu_o} \quad \text{(Reynolds number)}$$

and

$$Pr = \frac{\mu_o c_{vo}}{k_o}$$

$$E = \frac{u_o^2}{c_{vo} T_o}$$

Due to the non-dimensionalizing process all flow variable groups are now of order unity, and we must investigate the order of magnitude of the dimensionless parameters Re, Pr and E. While Pr is generally of order unity for all gases, it can be shown that, for the conditions in the laser heated thruster, the Reynolds number is also of order unity, while E is several orders of magnitude smaller. We can conclude that all terms are of equal importance in the continuity and momentum equations, but in the energy equation, however, the pressure terms, all carrying the E as a multiplier, will be orders of magnitude smaller than the convection and conduction terms.

In pursuit of a simple analytic solution we now examine steady state, inviscid one-dimensional flow at constant pressure. With these assumptions, the governing equations reduce to

Continuity:

$$\frac{d}{dx}(\rho u) = 0 \tag{21}$$

Energy:

$$\frac{d}{dx}\left[\rho u \left(\mathcal{E} + \frac{p}{\rho}\right) - k \frac{dT}{dx}\right] = Q \tag{22}$$

Recognizing that ($\mathcal{E} + p/\rho$) represents the total anthalpy which, for our case, consists of mostly thermal energy, we ignore the kinetic energy and write

$$\mathcal{E} + \frac{p}{\rho} = H \approx h = cp\,T + \text{constant} \tag{23}$$

Knowing that the GIM code presently requires c_p and k to be constant, the energy equation reduces to

$$\frac{d^2T}{dx^2} - \frac{\rho u\, c_p}{k}\frac{dT}{dx} = -\frac{Q}{k} \tag{24}$$

where, from Eq. (13)

$$Q = \alpha I_o e^{-\alpha x} - mk(T - T_i) \tag{25}$$

Of course, this ordinary differential equation for T(x) is almost the same equation used by Raizer (op, cit.) except that we further simplified it by introducing an integrated average k and by neglecting radial conduction. As a matter of fact, we can easily include radial conduction in the same manner as Raizer did by modifying the constant m in the plasma radiation loss term.

We can rewrite the differential equation as

$$\frac{d^2T}{dx^2} - a\frac{dT}{dx} - mT = -\frac{P}{k}\, e^{-\alpha x} - mT_i \tag{26}$$

and arbitrarily specify that the laser power density $P = \alpha_o I_o$ obeys

$$P = 0 \quad \text{for } x < 0$$

$$P = P_o \quad \text{for } x \geq 0$$

such that $x = 0$ designates the location of plasma ignition (onset of ionization and laser energy absorption). Solutions are then obtained separately for $x < 0$ and $x > 0$, and the solutions T_1 and T_2 are joined by requiring that both T and its derivative match at $x = 0$. Thus, the boundary conditions take the following form:

$$x = 0: \qquad T_1 = T_2 = T_o$$

$$\frac{dT_1}{dx} = \frac{dT_2}{dx} ,$$

$$x \longrightarrow -\infty \qquad T_1 = T_i$$

$$x \longrightarrow +\infty \qquad \frac{dT_2}{dx} = 0$$

Standard procedures for nonhomogeneous linear differential equations then yield for $x \leq 0$:

$$T_1(x) = (T_o - T_i)\, e^{\frac{a+b}{2}x} + T_1 \tag{27}$$

and for $x \geq 0$:

$$T_2(x) = C_1 e^{-\frac{b-a}{2}x} + C_2 e^{-\alpha x} + T_i \tag{28}$$

where

$$C_1 = -\frac{b+a+2\alpha}{b-a-2\alpha}\,(T_o - T_i) \tag{29}$$

$$C_2 = \frac{2b}{b-a-2\alpha}\,(T_o - T_i) \tag{30}$$

$$b \equiv \sqrt{a^2 + 4m} > 0 \tag{31}$$

Imposition of the boundary conditions on $T_2(x)$ generates an additional relationship for the laser power density as a function of a, b and α, i.e.,

$$P_o = \frac{2k\left[m - \alpha(\alpha + a)\right] b}{b - (a + 2\alpha)} \left(T_o - T_i\right) \tag{32}$$

The above equations show that the solution has one free parameter, namely the "ignition" temperature T_o. Alternatively we could consider the initial laser power density P_o as given and determine the ignition temperature T_o required to satisfy the boundary conditions.

Results for typical conditions represented by a, α, and m as used by Keefer (Ref. 15) are shown in Fig. 6. The initial temperature, T_i, was assumed to be 300 K, and the ignition temperature T_o was taken as 9000 K representing the onset of ionization for hydrogen at p = 1 atm (see Fig. 5). The temperature distribution through the laser absorption wave is in excellent qualitative agreement with results obtained by Keefer (Ref. 15) for the same choice of parameters. Of course, since our results represent a strictly one-dimensional situation (i.e., radial conduction and finite laser beam dimensions are ignored), exact quantitative agreement with Keefer's results cannot be expected.

Another point learned from this one-dimensional exercise is that, without the explicit inclusion of the radiation loss term in the differential equation, the differential equation does not have a solution which is able to satisfy the downstream boundary conditions. Both the temperature and its derivative will become infinite as x approaches infinity, i.e., the solution diverges. Even though the full conservation equations used in the GIM code contain the radial conduction term, and therefore provide an energy loss

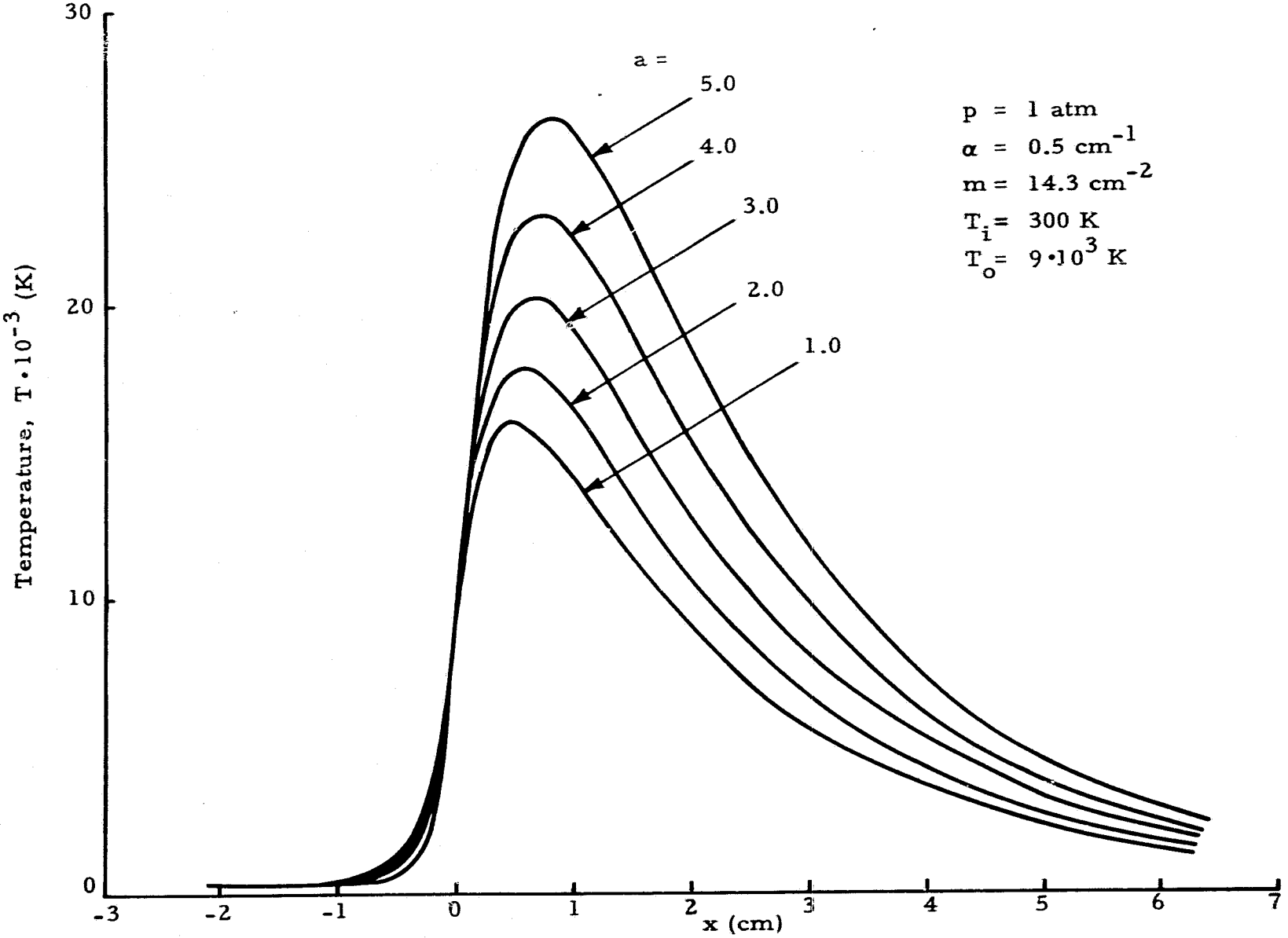

Fig. 6 - Temperature Distribution Through Absorption Wave (Hydrogen at p = 1 atm)

term, this may not be of sufficient magnitude to prevent the temperature from reaching unreasonable values. As can be seen from the example presented by Keefer, the power loss due to plasma radiation far outweighed that due to thermal conduction in the radial direction.

The purpose of investigating this simplified analytical model, although it duplicates to some degree work previously accomplished, was to provide insights which should be of help to obtain a solution from the GIM code. This will be discussed in the following section.

4.3 TWO-DIMENSIONAL FLUID MECHANICS EFFECTS

The successful use of detailed numerical methods such as those used in the GIM code requires careful planning with regard to grid selection, initial values and boundary conditions, time step selection and possibly scaling considerations to accelerate convergence.

The analytical results shown in the previous section (as well as Keefer's results) show that we have to deal with very steep temperature gradients in the laser absorption wave. This immediately suggests a rather tight spatial grid, but how tight? Selecting too coarse a grid can generate oscillations in the solution; but too fine a grid will be costly in terms of computation time and storage.

Using a time-dependent method for the computation of subsonic flow fields, particular care must be exercised in order to ensure that boundary conditions remain well defined during the course of the calculation. The laser heated thruster is modeled as a straight circular duct with vanishing velocity at the wall, specified uniform velocity at the inflow boundary and an outflow velocity distribution to be determined by the analysis. In order to keep the problem defined, the laser absorption wave must be positioned far enough downstream from the subsonic inflow boundary such that the latter is not subjected to changes caused by the upstream influence exerted by the former. The analytic solution discussed previously shows that, for the

sample conditions chosen, the laser absorption wave must be positioned in the duct no closer than approximately two cm to the inflow boundary (see Fig. 6), assuming that the analytical solution is quantitatively correct with respect to gradients expected in the axial direction.

Initial conditions, and average values for thermodynamic and transport properties must be chosen carefully to be representative of the enormous temperature range that has to be covered (with constant values) and, simultaneously, they must be consistent in representing the parameters used in the calculations with which we want to compare the GIM code results, viz.

$$\frac{\rho u\, c_p}{k} = a = 5.0\ \text{cm}^{-1} \tag{33}$$

$$\frac{c_p}{k} = 2.75 \cdot 10^3\ \text{cm sec/g} \tag{34}$$

A consistent set of variables can be selected as follows: According to Keefer's results we expect a maximum temperature of around $20 \cdot 10^3$ K. From Fig. 4 it is found that an integrated average value for the specific heat covering this temperature range is $\overline{c_p} = 110$ J/gK. The given ratio of $\overline{c_p}/\overline{k}$ then yields $\overline{k} = 4.0 \cdot 10^{-2}$ J/cm sec K, a reasonable value as can be seen from Fig. 3. While the analytic solutions are determined on the basis of global parameters such as $\rho u\, c_p/k$, the GIM code requires specification of these variables separately. In fact, the GIM code uses γ and R to compute the specific heat. Selecting an integrated average of R = 9.4 J/gK from Fig. 5, we can compute the ratio of specific heats to be $\gamma = 1.094$. The equation of state and Eq. (34) then yield $\rho = 3.593 \cdot 10^{-5}$ g/cm^3 and u = 50.602 cm/sec, assuming p = 1 atm and T = 300 K as initial conditions.

The selection of the spatial grid for this problem (21 stations in the axial direction, 26 points in the radial direction) represents a compromise

between anticipated requirements concerning resolution and the limitations of the MSFC Univac 1100 system with respect to computational speed and data storage.

Pure flow calculations without laser energy addition were performed first. Results from these can be checked against exact (i.e., analytical) solutions for axisymmetric Poiseuille flow. Initial calculations with a time increment as dictated by the CFL criterion showed extremely slow convergence. Much faster convergence was eventually realized by scaling the problem. Scaling as applied here involves multiplication of key variables, i.e., the velocity, the viscosity and the thermal conductivity in this case, by a scale factor ($1 \cdot 10^3$, typically) such that Reynolds number and Prandtl number are preserved. This type of scaling does increase the Mach number. However, because of the rather small velocity, even the scaled Mach number remains much smaller than unity, and therefore the basic subsonic flow character of the problem is preserved.

Typical results are shown in Figs. 7 and 8. As seen in Fig. 7, the initial velocity profile is uniform (over the entire spatial domain) except for the velocity at the wall which is set to zero. As the parabolic velocity profile developes in time along the channel, its magnitude in the outflow plane is continually adjusted by mass balance considerations. This adjustment causes a feed-back into the interior of the flow field and thereby enhances convergence of the solution. Figure 7 shows the outflow velocity profile to have the proper parabolic distribution with a maximum velocity on the centerline at roughly twice the value of the average velocity (as represented by the inflow velocity distribution) as predicted by the exact solution. A complete velocity vector plot is presented in Fig. 8 which very clearly shows the contraction and acceleration of the flow in the interior of the channel due to the boundary layer developing along the channel wall.

These results also demonstrate well the viscous nature of the flow. Note that the scaling factor applied does not affect the balance between

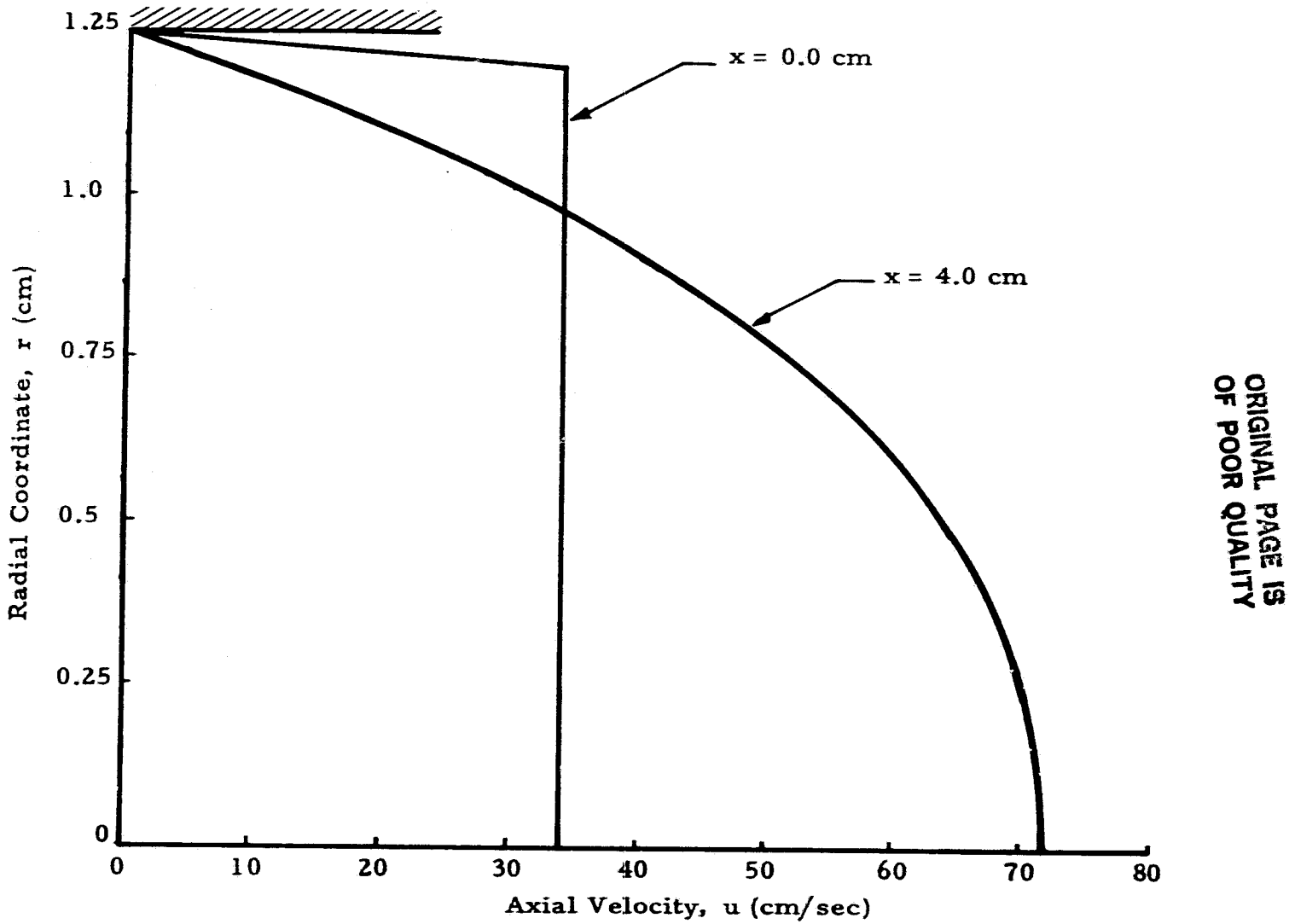

Fig. 7 - Axial Velocity Distribution in Axisymmetric Flow Channel (without laser heating)

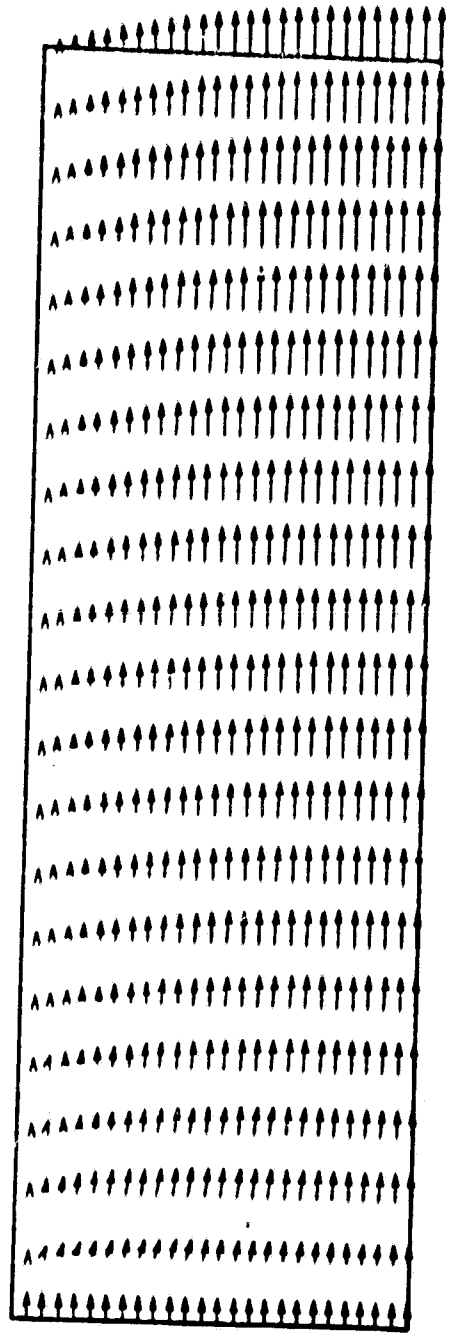

Fig. 8 - Velocity Vectors in Axisymmetric Flow Channel ($\Delta t = 5 \cdot 10^{-8}$ sec, Iteration No. 500, Scale Factor = $1 \cdot 10^{3}$)

viscous and inertial forces because the Reynolds number is preserved. When introducing the scaling factor into the equations it can be seen that its effect is to increase the viscous dissipation terms relative to the convection and conduction terms in the energy equation. This gives the scaling factor basically the function of a convergence accelerator, particularly so since it was shown previously that the dissipation terms are negligible for very slow flows, and remain so in spite of the scale factor. Typical calculations involving a time step of $\Delta t = 1 \cdot 10^{-7}$ sec, and a thousand time steps to obtain a converged solution require about one hour of Univac 1100 computer time.

All efforts to obtain a numerical solution for the flow with laser heating were unsuccessful. In order to gain an understanding why solutions could not be obtained, it is useful to take a closer look at the time step criteria which must be observed to control the stability of the numerical calculations. The first one is the CFL condition, which can be expressed as

$$\Delta t_{CFL} \leq \frac{\Delta}{|u| + a} \tag{35}$$

where Δ is the smallest spatial grid spacing used, and a is the speed of sound. The second is a thermal stability criterion, which, when specialized to flows with constant pressure (which is very nearly true for our case), reads

$$\Delta t_T \leq \frac{1}{2} \left(\frac{p}{RT}\right) \left(\frac{c_p}{k}\right) \frac{1}{\Delta x^{-2} + \Delta r^{-2}} \tag{36}$$

Specialized to our case for constant properties and grid spacings of Δx = 0.2 cm and Δr = 0.05 cm, these criteria become

$$\Delta t_{CFL} \leq 2.25 \cdot 10^{-7} \sqrt{\frac{300}{T}} \quad \text{(sec)} \tag{37}$$

$$\Delta t_{T} \leq 1.16 \cdot 10^{-7} \left(\frac{300}{T}\right) \text{(sec)} \tag{38}$$

It is immediately evident that Δt_T presents the more stringent criterion, especially for flows with high temperatures as they are expected in the laser heated propulsion problem. Since typical cases, using $\Delta t = 1 \cdot 10^{-7}$ (sec) require about one hour to converge on the Univac 1100, a temperature rise to about 20,000 K will reduce the permissible time step by nearly two orders of magnitude. Assuming that the total time required to obtain a converged solution remains the same as before, we are faced with computer times of the order of a hundred hours per case. This is clearly an impossible proposition. The only remedy here appears to be a computer such as the STAR or the CRAY, both of which can better handle the storage requirements imposed by this problem, and both of which work at much faster computational speed. Additional computational time savings can most likely be realized by utilizing a variable time step to be evaluated as a function of temperature as given by the time step criteria. This feature is included in the GIM code version for the STAR computer. Unfortunately, the latter (with its GIM code version tailored to it) was not available for this study.

5. CONCLUSIONS

The numerical analysis of two-dimensional fluid mechanics effects in the laser heated thruster is characterized by low density, very high temperatures and extremely large gradients in both variables. Because of subsonic flow throughout, the governing equations are of the elliptic type and require a solution by a time relaxation method with extremely small step sizes in time as dictated by the stability criteria. The first prerequisite for a successful solution of this problem therefore is a computer facility which can handle the storage requirements and is sufficiently fast so that the problem can be solved in reasonable time. The Univac 1100 system does not meet these requirements.

Simplified analytical solutions have shown that there exists a particular relationship between the gas flow velocity and the laser power which the flow can absorb and simultaneously satisfy the downstream boundary condition of a finite temperature. While this relationship is easily obtained as part of the analytical solution of the simplified equations, most likely it can only be satisfied in a numerical solution via an iterative approach. This implies repetitive calculations and therefore amplifies the requirements for a large and fast computer.

Numerical solutions of subsonic flow problems via time dependent methods require particular attention to the specification of boundary conditions at the inflow and outflow boundaries. This is a subject of current research. It is not known at present to what extent the lack of appropriate boundary conditions has contributed to the failure of the present effort.

The fact that the GIM code version usable on the Univac 1100 system is restricted to constant thermodynamic and transport properties should by

itself not prevent a solution. Clearly though, when the temperature varies to the extent as it does in the laser heated thruster problem, the use of temperature dependent properties would appear to be more realistic.

Finally, considering the critical dependence of the permissible time step on the temperature, any future attempts at solving the flow problems in the laser heated thruster should use a variable time step methodology in order to minimize computer time (and cost).

REFERENCES

1. Hughes, T.P., Plasmas and Laser Light, Wiley, New York, 1975.

2. Raizer, Y.U., Sov. Phys. JETP, Vol. 31, 1970, p. 1148.

3. Jackson, J.T., and P.E. Nielsen, "Role of Radiative Transport in the Propagation of Laser Supported Combustion Waves," AIAA J., Vol. 12, 1974, p. 1498.

4. Batteh, J.H. and D.R. Keefer, "Two-Dimensional Generalization of Raizer's Analysis for the Subsonic Propagation of Laser Sparks," IEEE Transaction of Plasma Science, PS-2, September 1974.

5. Kemp, N.H., and R.G. Root, "Analytical Study of Laser Supported Combustion Waves in Hydrogen," PSI TR-97 (NASA CR-135349), Physical Sciences, Inc., August 1977.

6. Klosterman, E.L., and S.R. Byron, "Measurement of Subsonic Laser Absorption Wave Propagation Characteristics at 10.6 m," AIAA J., Vol. 12, 1974, p. 1498 (cited in Ref. 3).

7. Conrad, R.W., "Plasma Initiation and Propagation with a High Power, CW, CO_2 Laser," U.S. Army Missile Command Report RR-TR-72-8, June 1972 (SECRET).

8. Kemp, N.H., and P.F. Lewis, "Laser-Heated Thruster - Interim Report," PSI TR-205 (NASA CR-161665), Physical Sciences, Inc., February 1980.

9. Kemp, N.H., and R.H. Krech, "Laser-Heated Thruster - Final Report," PSI TR-220 (NASA CR-161666), Physical Sciences, Inc., September 1980.

10. Park, Chul, "Calculation of Radiative Properties of Nonequilibrium Hydrogen Plasma," J. Quant. Spectrosc. Radiat. Transfer, Vol. 22, 1979, p. 101.

11. Kruger, C.H., and M. Mitchner, "Kinetic Theory of Two-Temperature Plasmas," The Physics of Fluids, Vol. 10, No. 9, September 1967, p. 1953.

12. Rawlinson, E.G., M.A. Robinson and L.W. Spradley, "GIM Code User's Manual," LMSC-HREC TR D7840 , Lockheed Missiles & Space Company, Huntsville, Ala., January 1981.

13. Patch, R.W., "Thermodynamic Properties and Theoretical Rocket Performance of Hydrogen to 100,000 K and 1.01325 x 10^8 N/m^2," NASA SP-3069 (1971).

14. Svehla, Roger A., "Estimated Viscosities and Thermal Conductivities of Gases at High Temperatures," NASA TR R-132 (1962).

15. Keefer, D.R., H. Crowder, R. Elkins and R. Eskridge," Laser Heated Rocket Analytical and Experimental Support," Final Report, Subcontract SM80C1160F, University of Tennessee Space Institute, July 1981.